

THE GALERKIN METHOD SOLUTION OF THE CONJUGATE HEAT TRANSFER PROBLEMS FOR THE CROSS-FLOW CONDITIONS

Andrej Horvat

ANSYS CFX
Harwell International Business Centre
Fermi Avenue
Didcot, Oxfordshire, OX11 0QR
United Kingdom

Borut Mavko

Reactor Engineering Division
"Jožef Stefan" Institute
Jamova 39
Ljubljana, SI-1001
Slovenia

Ivan Catton

Mechanical and Aerospace Engineering Department
The Henry Samueli School of Engineering and Applied Science
University of California, Los Angeles
Los Angeles, California, 90095-1597
United States of America

ABSTRACT

A conjugate heat transfer model of fluid flow across a solid heat conducting structure has been built. Two examples are presented: a.) air-stream cooling of the solid structure and b.) flow across rods with volumetric heat generation. To construct the model, a Volume Average Technique (VAT) has been applied to the momentum and the energy transport equations for a fluid and a solid phase to develop a specific form of porous media flow equations. The model equations have been solved with the semi-analytical Galerkin method.

The detailed velocity and temperature fields in the fluid flow and the solid structure have been obtained. Using the solution fields, the whole-section drag coefficient C_d and the whole-section Nusselt number Nu have been also calculated. To validate the developed solution procedure, the results have been compared to the results of the finite volume method and to the experimental data. The comparison demonstrates an excellent agreement.

INTRODUCTION

Heat transfer conditions in a heat exchanger are a well known and extensively studied subject. Also, today available computational power gives us an opportunity to build increasingly detailed physical models of heat transfer processes. Nevertheless, direct computations of whole heat exchanger installations are at present still far from an everyday engineering practice. In order to resolve most of the flow features and at the same time keep the model simple enough to serve as an engineering tool, averaging of fluid and heat flow variables has to be performed.

A Volume Averaging Technique (VAT) has been developing from the 1960s and it has been applied to a number of different fluid dynamics and heat transfer problems. Recently, it has been applied to model processes in heat exchangers and heat sinks (Hu, 2001, Horvat & Catton, 2001 & 2003). Using VAT, the transport processes in a heat exchanger are modeled as porous media flow (Travkin & Catton, 1999). This generalization allows us to unify the heat transfer calculation techniques for different kinds of heat exchangers and their structures. The case-specific geometrical arrangements, material properties and fluid flow conditions enter the computational algorithm only as a series of precalculated coefficients. The

clear separation between the model and the case-specific coefficients simplifies the model and speeds up calculations.

In most cases, the developed set of VAT equations has been solved with the finite difference or the finite volume method. Lately, efforts have been made to obtain the solution also by the Galerkin method (Horvat & Catton, 2003).

The Galerkin method is a semi-analytical method, where a solution field is anticipated to be a series of orthogonal functions. As the solution depends only on a number of orthogonal functions and not on a number of grid nodes, highly accurate solutions can be obtained. In the present paper, two applications of the Galerkin method are given. In the first case, we present a closed-form solution for the conjugate heat transfer problem of air-stream cooling of a solid structure. In the second case, a solution for water flow across rods with volumetric heat generation is given. Although the Galerkin method has limited applicability in complex geometries, its highly accurate solutions are an important benchmark on which other numerical results can be tested. Further, the VAT formulation lends itself to the Galerkin method because most of the geometric complexity is absorbed into the closure relationships.

GEOMETRY LAYOUT

For both cases (i.e. the air-stream cooling of the solid structure and the flow across rods with volumetric heat generation), a similar geometry has been used (Fig. 1).

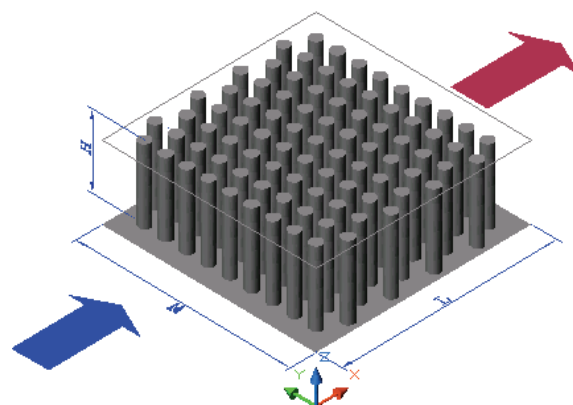


Figure 1: General geometrical layout

A cold stream of fluid enters from the left and is heated by the solid structure as it passes the test section. The flow is bounded at the bottom by an isothermal wall, where no-slip boundary conditions are prescribed. At the top, the flow is considered open. The details on boundary conditions for each specific case will be given later.

In the first case, the length L as well as the width W of the aluminum solid structure are 11.43 cm, whereas the height H is 3.81 cm. The simulation domain consists of 31 rows of pin-fins in the streamwise direction and 31 rows of pin-fins in the transverse direction. The diameter of the pin-fins d is 0.3175 cm. A pitch-to-diameter ratio in the streamwise direction p_x/d is set to 1.06 and in the transverse direction p_y/d is 2.12.

In the second case, the aluminum rods with internal heat generation rate I have a diameter d of 0.9525 cm. Their height is 20 cm. They are arranged in 64 rows in the streamwise direction and in 16 rows in the transverse direction. In the streamwise direction, a pitch-to-diameter ratio p_x/d is 1.0 and in the transverse direction p_y/d is 2.0. At the bottom, the rods are attached to an isothermal plate that is 60.96 cm long and 30.48 cm width.

In both cases, the entering flow profile is assumed to be fully developed.

MATHEMATICAL MODEL

Flow across a solid structure can be described with basic mass, momentum and heat transport equations (Horvat, 2002). In order to develop a unified approach for different geometries and material properties, the transport equations are averaged over a representative elementary volume (Fig. 2).

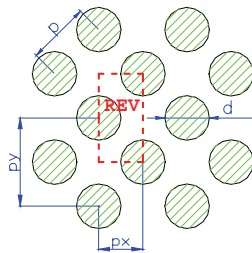


Figure 2: Representative elementary volume

This volume averaging leads to a closure problem where interface exchange of momentum and heat between a fluid and a solid has to be described with additional empirical relations e.g. a local drag coefficient f and a local heat transfer coefficient h . Reliable data for the local drag coefficient f and the heat transfer coefficient h have been found in Launder & Massey (1978), Žukauskas & Ulinskas (1985), and Kays & London (1998).

In both cases, the simulated system has been further simplified by assuming flow with a dominating streamwise velocity component and a constant pressure drop across the structure. As a consequence, the velocity changes only vertically in the z -direction. This means that the streamwise pressure gradient across the entire simulation domain is balanced with the hydrodynamic resistance of the structure and with the shear stress. Thus, the momentum equation can be written in the differential form as

$$-\alpha_f \hat{\rho}_f \frac{\partial^2 \hat{u}}{\partial \hat{z}^2} + \frac{1}{2} f \hat{\rho}_f \hat{u}^2 \hat{S} = \frac{\Delta \hat{p}}{\hat{L}} \quad (1)$$

The energy transport equation for the fluid flow has also been developed using the unidirectional velocity assumption. The temperature field in the fluid results from the balance between thermal convection in the streamwise direction, thermal diffusion and the heat transferred from the solid structure to the fluid flow:

$$\alpha_f \hat{\rho}_f \hat{c}_f \hat{u} \frac{\partial \hat{T}_f}{\partial \hat{x}} = \alpha_f \hat{\lambda}_f \frac{\partial^2 \hat{T}_f}{\partial \hat{z}^2} - \hat{h}(\hat{T}_f - \hat{T}_s) \hat{S} \quad (2)$$

The rod bundle structure in each REV is not connected in the horizontal directions (see Fig. 1). As a consequence, only the internal heat generation I and the thermal diffusion in the vertical direction are in balance with the heat leaving the structure through the fluid-solid interface. The thermal diffusion in the horizontal directions can be neglected. This simplifies the energy equation for the solid structure to:

$$0 = \alpha_s \hat{\lambda}_s \frac{\partial^2 \hat{T}_s}{\partial \hat{z}^2} + \hat{h}(\hat{T}_f - \hat{T}_s) \hat{S} + \alpha_s \hat{I} \quad (3)$$

In the case of the air-stream cooling of the solid structure, the last term is zero as there is no volumetric heat generation in the solid structure.

Boundary conditions for the set of equations (1-3) are given below

$$\begin{aligned} \hat{x}=0 : \quad & \hat{T}_f = \hat{T}_{in} \quad , \quad (4) \\ \hat{z}=0 : \quad & \hat{u}=0, \quad \hat{T}_f = \hat{T}_g, \quad \hat{T}_s = \hat{T}_g \quad , \\ \hat{z}=\hat{H} : \quad & \hat{u}=0, \quad \frac{\partial \hat{T}_f}{\partial \hat{z}} = 0, \quad \frac{\partial \hat{T}_s}{\partial \hat{z}} = 0 \quad , \end{aligned}$$

and are valid for both cases.

SOLUTION METHOD

To construct the solution method, the transport equations (1-3) have been scaled and converted into a dimensionless form:

$$-M_2 \frac{\partial^2 u}{\partial z^2} + M_3 u^2 = M_4 \quad (5)$$

$$F_1 u \frac{\partial T_f}{\partial x} = F_4 \frac{\partial^2 T_f}{\partial z^2} - F_5 (T_f - T_s) \quad (6)$$

$$0 = S_1 \frac{\partial^2 T_s}{\partial z^2} + S_2 (T_f - T_s) - S_3 \quad (7)$$

where $M_2, M_3, M_4, F_1, F_4, F_5, S_1, S_2$ and S_3 are constants. In the same way, the boundary conditions (4) have been transformed to

$$\begin{aligned} x=0 : \quad & T_f = 1 \quad , \quad (8) \\ z=0 : \quad & u=0, \quad T_f = 0 \quad , \quad T_s = 0 \quad , \\ z=1 : \quad & u=0, \quad \frac{\partial T_f}{\partial z} = 0, \quad \frac{\partial T_s}{\partial z} = 0 \quad . \end{aligned}$$

The momentum equation (5) has the same form and the same boundary conditions in both cases. To obtain its solution, the momentum equation has been linearized to:

$$-M_2 \frac{\partial^2 u}{\partial z^2} + Ku = M_4, \tag{9}$$

where $K = M_3 |u|$. Taking into account the boundary conditions (8), the solution of Eq. (9) is:

$$u = G_1 \exp(\varepsilon z) + G_2 \exp(-\varepsilon z) + G_3. \tag{10}$$

The solution has the same form in both cases with different values of the constants ε, G_1, G_2 and G_3 .

Although the principles of the Galerkin method are the same for both cases, the differences in the solution procedure for the energy equations (6 & 7) require a separate treatment for each case.

Air-Stream Cooling of the Solid Structure

To find a solution to the conjugate problem, both equations (6 & 7) are combined into a single expression for the solid phase temperature T_s :

$$D_1 u \frac{\partial T_s}{\partial x} + D_2 \frac{\partial^4 T_s}{\partial z^4} - D_3 \frac{\partial^2 T_s}{\partial z^2} - D_4 u \frac{\partial^3 T_s}{\partial x \partial z^2} = 0, \tag{11}$$

where D_1, D_2, D_3 and D_4 are constants. Further, separation of variables is used:

$$T_s = X(x)Z(z). \tag{12}$$

where the solution in the z -direction is anticipated in the form of a series:

$$Z = A_k Z_k, Z_k = \sin(\gamma_k z), \gamma_k = \frac{2k-1}{2} \pi, k=1, n, \tag{13}$$

to satisfy the boundary conditions (8). Introducing (13) into (11) and regrouping the expression, we can write

$$X' A_k u \{D_1 + \gamma_k^2 D_4\} Z_k + X A_k \{\gamma_k^4 D_2 + \gamma_k^2 D_3\} Z_k = error. \tag{14}$$

As the series is finite, there is a certain discrepancy associated with the series expansion (14). This error is orthogonal to the set of functions used for the expansion and can be reduced by multiplying the equation (14) with Z_j ($j=1, n$) and integrating it from 0 to 1:

$$X' A_k \int_0^1 u \{D_1 + \gamma_k^2 D_4\} Z_k Z_j dz + X A_k \int_0^1 \{\gamma_k^4 D_2 + \gamma_k^2 D_3\} Z_k Z_j dz = 0. \tag{15}$$

In a matrix form, Eq. (15) is written as

$$X' A_k J_{kj}^{(1)} + X A_k J_{kj}^{(2)} = 0, \tag{16}$$

where $J_{kj}^{(1)}$ and $J_{kj}^{(2)}$ are integrals that are calculated analytically. As the x and z dependent parts of Eq. (16) can be separated:

$$\beta = -\frac{X'}{X} = \frac{A_k J_{kj}^{(2)}}{A_k J_{kj}^{(1)}}, \tag{17}$$

separate equations are written for the x -direction:

$$X' + \beta X = 0, \tag{18}$$

and for the z -direction:

$$(J_{kj}^{(2)} - \beta J_{kj}^{(1)}) A_k = 0. \tag{19}$$

The solution of Eq. (18) is obtained by integration:

$$X = C \exp(-\beta x), \tag{20}$$

where C and β are arbitrary constants.

Equation (19) is an extended eigenvalue problem that has non-trivial solutions if

$$\text{Det}(J_{kj}^{(2)} - \beta J_{kj}^{(1)}) = 0. \tag{21}$$

From the condition (21), a set of n eigenvalues β are determined. Furthermore, each eigenvalue β_j ($j=1, n$) corresponds to a specific j eigenvector A_k that is also calculated.

Using the solutions of Eq. (18) and of the matrix system (21), one can construct the temperature field for the solid phase:

$$T_s = C_j X_j A_{jk} Z_k, \tag{22}$$

and for the fluid phase:

$$T_f = C_j A_{jk} \left(1 + \frac{S_1}{S_2} \gamma_k^2 \right) Z_k, \tag{23}$$

where C_j is a vector of coefficients that is found from the boundary condition $T_f(0, z) = 1$. Applying it to Eq. (23), one can write:

$$C_j A_{jk} \left(1 + \frac{S_1}{S_2} \gamma_k^2 \right) Z_k = 1. \tag{24}$$

Again, multiplying Eq. (24) by Z_i ($i=1, n$) and integrating it from 0 to 1:

$$C_j A_{jk} \left(1 + \frac{S_1}{S_2} \gamma_k^2 \right) \int_0^1 Z_k Z_i dz = \int_0^1 Z_i dz, \tag{25}$$

the orthogonality condition reduces Eq. (25) to

$$C_j A_{ji} \left(1 + \frac{S_1}{S_2} \gamma_i^2 \right) J_i^{(1)} = J_i^{(2)}, \tag{26}$$

where $J_i^{(1)}$ and $J_i^{(2)}$ are analytically calculated integrals. Writing Eq. (26) in a matrix form:

$$C_j A_{ji} = \frac{J_i^{(2)}}{\left(1 + \frac{S_1}{S_2} \gamma_i^2 \right) J_i^{(1)}}, \tag{27}$$

the unknown coefficients C_j are calculated by inversion of the matrix system (27).

Flow Across Rods with Volumetric Heat Generation

In the case of internal heat generation in the solid structure, Eq. (11) has an additional term:

$$D_1 u \frac{\partial T_s}{\partial x} + D_2 \frac{\partial^4 T_s}{\partial z^4} - D_3 \frac{\partial^2 T_s}{\partial z^2} - D_4 u \frac{\partial^3 T_s}{\partial x \partial z^2} + D_5 = 0, \tag{28}$$

which significantly complicates the solution procedure. The solid-phase temperature field T_s needs to be separated as

$$T_s(x, z) = T_b(z) + t_s(x, z), \tag{29}$$

where T_b is a temperature field in absence of forced convection across the rod bundle ($u = 0$) and t_s is a solid-phase temperature residue. Inserting the decomposition (29) into Eq. (28), a separate equation is written for the temperature T_b :

$$D_2 \frac{\partial^4 T_b}{\partial z^4} - D_3 \frac{\partial^2 T_b}{\partial z^2} + D_5 = 0, \tag{30}$$

and for the temperature t_s :

$$D_1 u \frac{\partial t_s}{\partial x} + D_2 \frac{\partial^4 t_s}{\partial z^4} - D_3 \frac{\partial^2 t_s}{\partial z^2} - D_4 u \frac{\partial^3 t_s}{\partial x \partial z^2} = 0. \tag{31}$$

The boundary conditions (4) are transformed to

$$\begin{aligned} x=0: & \quad t_s = 1, \\ z=0: & \quad t_s = 0, \quad T_b = 0, \\ z=1: & \quad \frac{\partial t_s}{\partial z} = 0, \quad \frac{\partial T_b}{\partial z} = 0. \end{aligned} \tag{32}$$

A solution of Eq. (30) is found in the following form:

$$T_b = B_1 \exp(\xi z) + B_2 \exp(-\xi z) + B_3 + B_4 z + B_5 z^2, \tag{33}$$

where $\xi, B_1, B_2, B_3, B_4,$ and B_5 are constants to be determined from the boundary conditions (32).

Equation (31) has the same form as Eq. (28) in the previous case. Therefore, separation of variables is used:

$$t_s = X(x)Z(z). \tag{34}$$

Again, the solution for the z -direction of Eq. (31) is expressed as a finite set of n orthogonal functions:

$$Z = A_k Z_k, \quad Z_k = \sin(\gamma_k z), \quad \gamma_k = \frac{2k-1}{2} \pi, \quad k=1, n, \tag{35}$$

and the procedure to find $X(x)$ and $Z(z)$ is the same as in the previous case (Eqs. 14-21). Finally, the solution for temperature t_s can be expressed as:

$$t_s = C_j X_j A_{jk} Z_k, \tag{36}$$

where C_j is a vector of coefficients that has to be determined. Adding the temperature fields T_b (Eq. 33) to t_s (Eq. 36), the expression for the dimensionless solid-phase temperature T_s is written as

$$T_s = (B_1 \exp(\xi z) + B_2 \exp(-\xi z) + B_3 + B_4 z + B_5 z^2) + C_j X_j A_{jk} Z_k. \tag{37}$$

Recalling Eq. (7) and inserting the expression for the solid-structure temperature T_s (Eq. 37), the dimensionless fluid temperature is given by

$$\begin{aligned} T_f = & C_j A_{jk} \left(1 + \frac{S_1}{S_2} \gamma_k^2 \right) Z_k \\ & + B_1 \left(1 - \frac{S_1}{S_2} \xi^2 \right) \exp(\xi z) + B_2 \left(1 - \frac{S_1}{S_2} \xi^2 \right) \exp(-\xi z) \\ & + \left(B_3 - 2B_5 \frac{S_1}{S_2} + \frac{S_3}{S_2} \right) + B_4 z + B_5 z^2 \end{aligned} \tag{38}$$

The coefficients C_j are found with help of the boundary condition $T_f(0, z) = 1$. Imposing it onto Eq. (38), the following form is obtained:

$$\begin{aligned} C_j A_{jk} \left(1 + \frac{S_1}{S_2} \gamma_k^2 \right) Z_k = & B_1 \left(\frac{S_1}{S_2} \xi^2 - 1 \right) \exp(\xi z) \\ & + B_2 \left(\frac{S_1}{S_2} \xi^2 - 1 \right) \exp(-\xi z) + \left(1 - B_3 + 2B_5 \frac{S_1}{S_2} - \frac{S_3}{S_2} \right) - B_4 z - B_5 z^2 \end{aligned} \tag{39}$$

Next, Eq. (39) is multiplied by orthogonal functions Z_i ($i=1, n$) and integrated from 0 to 1:

$$\begin{aligned} C_j A_{jk} \left(1 + \frac{S_1}{S_2} \gamma_k^2 \right) \int_0^1 Z_k Z_i dz = & B_1 \left(\frac{S_1}{S_2} \xi^2 - 1 \right) \int_0^1 \exp(\xi z) Z_i dz \\ & + B_2 \left(\frac{S_1}{S_2} \xi^2 - 1 \right) \int_0^1 \exp(-\xi z) Z_i dz \\ & + \left(1 - B_3 + 2B_5 \frac{S_1}{S_2} - \frac{S_3}{S_2} \right) \int_0^1 Z_i dz - B_4 \int_0^1 z Z_i dz - B_5 \int_0^1 z^2 Z_i dz \end{aligned} \tag{40}$$

Due to orthogonality of basis functions Z_i , the expression (40) is simplified to:

$$\begin{aligned} C_j A_{ji} \left(1 + \frac{S_1}{S_2} \gamma_i^2 \right) J_i^{(1)} = & B_1 \left(\frac{S_1}{S_2} \xi^2 - 1 \right) J_i^{(2)} + B_2 \left(\frac{S_1}{S_2} \xi^2 - 1 \right) J_i^{(3)} \\ & + \left(1 - B_3 + 2B_5 \frac{S_1}{S_2} - \frac{S_3}{S_2} \right) J_i^{(4)} - B_4 J_i^{(5)} - B_5 J_i^{(6)} \end{aligned} \tag{41}$$

where $J_i^{(1)}, J_i^{(2)}, J_i^{(3)}, J_i^{(4)}, J_i^{(5)}$ and $J_i^{(6)}$ are analytically calculated integrals. Writing Eq. (41) in the matrix form:

$$C_j A_{ji} = \frac{RHS}{\left(1 + \frac{S_1}{S_2} \gamma_i^2 \right) J_i^{(1)}} \tag{42}$$

the unknown coefficients C_j are calculated by inversion of the matrix system (42).

RESULTS AND DISCUSSION

The calculations have been performed for different pressure drops and thermal inputs (Table 1 & 2). The imposed pressure drop causes flow across the heated solid structure. As the structure is cooled, a steady temperature field is formed in the fluid as well as in the structure.

The results obtained with the Galerkin method have been compared with the results of the VAT model solved with the finite volume method, and in the first case also with the experimental data of Rizzi et al. (2001). Comparisons have been

made for the velocity field u , the temperature field in the fluid flow T_f and in the solid structure T_s . Further, the whole-section values of the drag coefficient C_d and the Nusselt number Nu have been compared with results from the finite volume method and with the experimental data.

Air-Stream Cooling of the Solid Structure

Calculations have been performed at heating power $Q=50W$, $125W$ and $220W$ to match the experimental data obtained by Rizzi et al. (2001). In this section we present only calculated values of the whole-section drag coefficient C_d and Nusselt number Nu for the heating power $Q = 125W$. It should be noted that although different heating power Q is used, there exists a similarity in force convection heat removal from the heat sink structure.

Simulations of the heat sink thermal behavior have been done for a range of pressure drops Δp and boundary temperatures T_{in} and T_g , that are summarized in Table 1.

Table 1: Boundary conditions - preset values.

No.	Δp [Pa]	T_{in} [°C]	T_g [°C]
1	5.0	23.0	103.8
2	10.0	23.0	74.6
3	20.0	23.0	58.8
4	40.0	23.0	48.2
5	74.7	23.2	41.8
6	179.3	23.2	35.7
7	274.0	23.0	33.6
8	361.1	22.8	32.3

For calculations performed with the Galerkin method, 34 mesh points in x - and 140 mesh points z -direction have been used to simulate heat transfer processes in the fluid- and the solid-phase. As the accuracy of the semi-analytical Galerkin method is essentially connected with the number of the orthogonal functions used for expansion, Eq. (22), 45 basis functions have been used in this case.

Based on the calculated velocity and temperature fields, the whole-section drag coefficient

$$C_d = 2 \frac{\Delta \hat{p} \hat{A}_\perp}{\hat{\rho}_f [\hat{u}]^2 \hat{A}_o} \tag{43}$$

and the whole-section Nusselt number

$$Nu = \frac{[\hat{Q}] \hat{d}_h}{([\hat{T}_s] - [\hat{T}_f]) \hat{A}_o \hat{\lambda}_f} \tag{44}$$

are estimated as functions of Reynolds number.

Figure 3 shows the whole-section drag coefficient C_d (Eq. 43) as a function of Reynolds number. The results calculated with the Galerkin method are close to the results obtained with the finite volume method as well as to the experimental data. Slight discrepancy from the experimental data at higher Reynolds number is due to transition to turbulence, which is evident on the experimental results, but is not captured by the model.

Figure 4 shows the whole-section Nusselt number Nu (Eq. 44), as a function of Reynolds number. The differences between the Galerkin method results, the finite volume method results

and the experimental data are negligible as the Reynolds number increases from $Re = 762$ to $Re = 1893$.

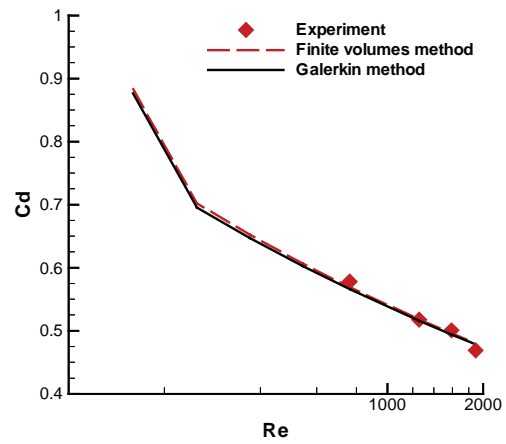


Figure 3: Whole-section drag coefficient C_d , 125W

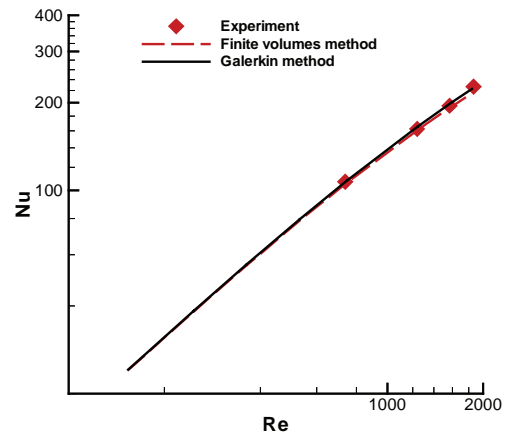


Figure 4: Whole-section Nusselt number Nu , 125W

Flow Across Rods with Volumetric Heat Generation

Three sets of calculations of the water flow across the heat generating rod bundle have been performed for the volumetric heat generation rate of 0.0 W/cm^3 , 0.5 W/cm^3 and 2.0 W/cm^3 . Due to space limitations, only the results for the last case are presented. The boundary values of pressure drops Δp and temperatures T_{in} and T_g used in this case are summarized in Table 2.

Table 2: Boundary conditions - preset values.

No.	Δp [Pa]	T_{in} [°C]	T_g [°C]
1	40.0	35.0	39.0
2	80.0	35.0	39.0
3	120.0	35.0	39.0
4	160.0	35.0	39.0
5	200.0	35.0	39.0
6	240.0	35.0	39.0
7	280.0	35.0	39.0
8	320.0	35.0	39.0
9	360.0	35.0	39.0

All calculations with the Galerkin approach have been done with 80 eigenfunctions. For the finite volume method simulations, 64 grid points have been used in the x -direction, and 80 grid points in z -direction.

Although, the whole section drag coefficient C_d and the Nusselt number Nu have also been determined, we have chosen to present the comparison of the velocity and the temperature fields calculated with the Galerkin method and the finite volume method.

Figure 5 shows the velocity distributions obtained with the Galerkin method (marked as GM) and the finite volume method (marked as FVM). Note that the core of the simulation domain has a flat velocity profile due to the drag associated with the submerged rods. The results comparison reveals an excellent agreement between both methods, although the VAT momentum equation in the present Galerkin solver (Eq. 9) is simply linearized.

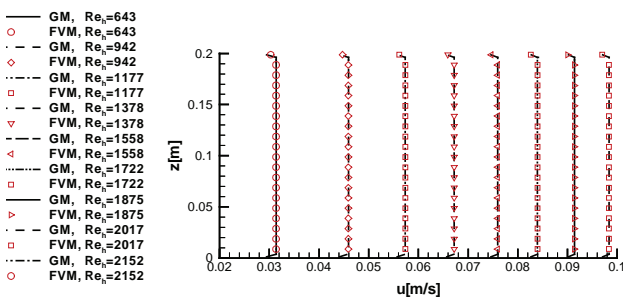


Figure 5: Velocity distribution for different Reynolds numbers

Figure 6 gives a temperature field cross-section in the water flow for the Reynolds number $Re = 2152$. The internal heat generation in the rods is set to $I = 2.0 \text{ W/cm}^3$. The temperature fields are presented in the Celsius scale. Bold isotherms denote the results obtained with the Galerkin method and half-tone (red) isotherms denotes temperatures obtained with the finite-volume method. Isotherms show that the fluid temperature increases in the horizontal direction, from the inflow to the outflow due to heat generating rods. Heating from the isothermal bottom is of minor importance.

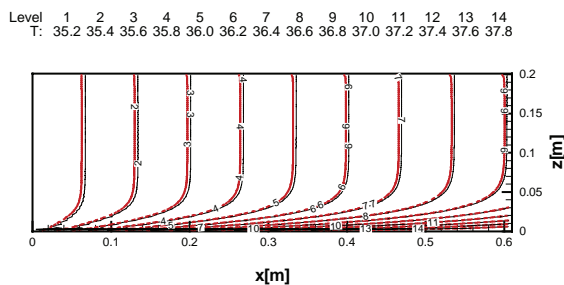


Figure 6: Temperature field in the water flow; $I = 2.0 \text{ W/cm}^3$, $Re = 2152$; (—) Galerkin method, (---) Finite volume method

Figure 7 shows the temperature in the aluminum structure. As the temperature of the fluid flow is higher at the exit than at the entrance, lack of cooling increases the temperatures in the solid structure. Due to higher thermal conductivity of the aluminum rods, the temperature field in the solid structure

reveals higher vertical gradients close to the isothermal bottom surface than in the water flow.

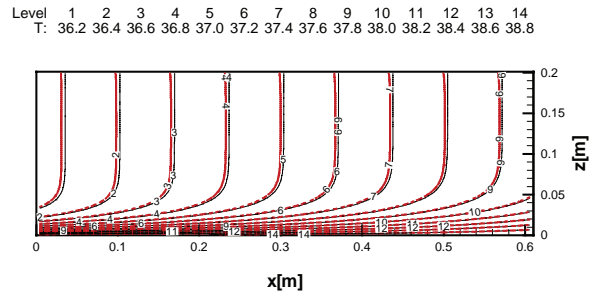


Figure 7: Temperature field in the solid rods; $I = 2.0 \text{ W/cm}^3$, $Re = 2152$; (—) Galerkin method, (---) Finite volume method

CONCLUSIONS

The paper presents an effort to utilize the Galerkin method for solving conjugate heat transfer problems in cross-flow condition.

In the scope of this work, the Volume Averaging Technique (VAT) was used to develop a specific form of the porous media flow models. The advantage of using VAT is that the computational algorithm is fast running, but still able to present a detailed picture of temperature fields in the fluid flow as well as in the solid structure.

The semi-analytical Galerkin procedure was developed to solve the system of equations. To show applicability of the Galerkin method, two examples were presented. In the first example, the velocity and the temperature fields were calculated for the air cooling of the aluminum heat sink. The second example showed the solution procedure for the flow across rods with volumetric heat generation.

The present paper gives only a part of results. Namely, for both cases, the whole-section drag coefficient C_d and the Nusselt number Nu were calculated and compared with the results of the finite volume method and in the first case also with the experimental data (Rizzi et al., 2001). The comparisons showed excellent agreement. The detailed velocity and temperature fields in the coolant flow as well as in the heat conducting structure were also calculated and compared with the results of the finite volume method. The comparisons show negligible differences between the results of both methods.

The present results demonstrate that the selected Galerkin approach is capable of solving thermal problems where the thermal conductivity and volumetric heat generation in the solid structure significantly influence the heat transfer and therefore have to be taken into account.

REFERENCES

Horvat, A. & Catton, I., 2001, Development of an Integral Computer Code for Simulation of Heat Exchangers, *Proc. Nuclear Energy in Central Europe 2001*, Portorož, Slovenia, Paper 213.

Horvat, A., 2002, Calculation of Conjugate Heat Transfer in a Heat Sink Using Volume Averaging Technique (VAT), M.Sc. Thesis, University of California, Los Angeles, USA.

Horvat, A. & Catton, I., 2003, Numerical Technique for Modeling Conjugate Heat Transfer in an Electronic Device Heat Sink, *Int. J. Heat Mass Transfer*, vol. 46, pp. 2155-2168.

Horvat, A. & Catton, I., 2003, Application of Galerkin Method to Conjugate Heat Transfer Calculation, *Numerical Heat Transfer B: Fundamentals*, vol. 44, No. 6, pp. 509-531.

Hu, K., 2001, Flow and Heat Transfer over Rough Surfaces in Porous Media, Ph.D. Thesis, University of California, Los Angeles, USA.

Kays, W.S. & London, A.L., 1998, *Compact Heat Exchangers*, 3rd Ed., Krieger Publishing Company, Malabar, Florida, pp. 152-155.

Launder, B.E. & Massey, T.H., 1978, The Numerical Prediction of Viscous Flow and Heat Transfer in Tube Banks, *J. Heat Transfer*, vol. 100, pp. 565-571.

Rizzi, M., Canino, M., Hu, K., Jones, S., Travkin, V., Catton, I., 2001, Experimental Investigation of Pin Fin Heat Sink Effectiveness, *Proc. 35th National Heat Transfer Conference*, Anaheim, California.

Travkin, V.S. & Catton, I., 1999, Transport Phenomena in Heterogeneous Media Based on Volume Averaging Theory, *Advans. Heat Transfer*, vol. 34, pp. 1-143.

Žukauskas, A. & Ulinskas, A., 1985, Efficiency Parameters for Heat Transfer in Tube Banks, *J. Heat Transfer Engineering*, vol. 5, No.1, pp. 19-25.

ACKNOWLEDGEMENTS

A. Horvat gratefully acknowledges the financial support received from the Kerze-Cheyovich scholarship and the Ministry of Higher Education, Science and Technology of RS under the project "Determination of morphological parameters for optimization of heat exchanger surfaces".

NOMENCLATURE

A_o	interface area [m ²]
A_{ji}	eigenvectors [dimensionless]
A_{\perp}	= $W \cdot H$, channel flow area [m ²]
B_1	= $(S_3/S_1 - 2B_5)/(1 + \xi^2 \exp(2\xi))$ [dimensionless]
B_2	= $B_1 \exp(2\xi)$ [dimensionless]
B_3	= $-B_1 - B_2$ [dimensionless]
B_4	= $-2B_5 - B_1 \xi \exp(\xi) + B_2 \xi \exp(-\xi)$ [dimensionless]
B_5	= $D_5/(2D_3)$ [dimensionless]
c_f	fluid specific heat [J/kgK]
C_d	drag coefficient [dimensionless]
d	diameter [m]
d_h	hydraulic diameter (= $4\Omega_f/A_o$) [m]
D_1	= F_1 [dimensionless]
D_2	= $F_4 S_1/S_2$ [dimensionless]
D_3	= $F_5 S_1/S_2 + F_4$ [dimensionless]

D_4	= $F_1 S_1/S_2$ [dimensionless]
D_5	= $F_1 S_3/S_1$ [dimensionless]
f	local drag coefficient [dimensionless]
F_1	= $\alpha_f c_f \rho_f U d_h/(\lambda_f L)$ [dimensionless]
F_4	= $\alpha_f d_h^2/H^2$ [dimensionless]
F_5	= $h d_h^2 S/\lambda_f$ [dimensionless]
G_1	= $-M_4/(K(1-\exp(\epsilon)))$
G_2	= $-G_1 M_4/K$
G_3	= M_4/K
h	heat transfer coefficient [W/m ² K]
I	volumetric heat generation rate [W/m ³]
J_{kj}	analytically calculated integrals [dimensionless]
K	= $M_3 u $ [dimensionless]
L	length of the simulation domain [m]
M_2	= $\alpha_f \mu_f d_h/(\rho_f U H^2)$ [dimensionless]
M_3	= $f d_h S/2$ [dimensionless]
M_4	= d_h/L [dimensionless]
Nu	Nusselt number [dimensionless]
p	pitch [m]
Δp	pressure drop across simulation domain [Pa]
Q	thermal power [W]
Re	Reynolds number (= $\rho_f u d_h/\mu_f$) [dimensionless]
RHS	right-hand-side of the equation
S	specific interface surface [1/m]
S_1	= $\alpha_s d_h^2/H^2$ [dimensionless]
S_2	= $h d_h^2 S/\lambda_s$ [dimensionless]
S_3	= $\alpha_s d_h^2 I/(\lambda_s(T_g - T_{in}))$ [dimensionless]
t_s	solid phase temperature residue [dimensionless]
T_b	solid phase temp. in absence of convection, [dimensionless]
T_f	fluid temperature [K], [dimensionless]
T_g	bottom temperature [K], [dimensionless]
T_{in}	inflow temperature [K], [dimensionless]
T_s	solid temperature [K], [dimensionless]
U	velocity scale (= $\sqrt{\Delta p/\rho_f}$) [m/s]

Greek letters

α_f	fluid fraction [dimensionless]
α_s	solid fraction (1- α_f) [dimensionless]
β	eigenvalues [dimensionless]
γ	= $\pi(2n-1)/2$ [dimensionless]
ϵ	= $\sqrt{K/M_2}$ [dimensionless]
Z	z - dependent part of T [dimensionless]
λ_f	fluid thermal conductivity [W/mK]
λ_s	solid thermal conductivity [W/mK]
ξ	= $\sqrt{D_3/D_2}$ [dimensionless]
X	x - dependent part of T [dimensionless]
Ω_f	fluid volume [m ³]